Pharm Res (2012) 29:953–960
DOI 10.1007/s11095-011-0635-y

RESEARCH PAPER

MR Molecular Imaging of Prostate Cancer with a Peptide-Targeted Contrast Agent in a Mouse Orthotopic Prostate Cancer Model

Mingqian Tan • Susan M. Burden-Gulley • Wen Li • Xueming Wu • Daniel Lindner • Susann M. Brady-Kalnay • Vikas Gulani • Zheng-Rong Lu

Received: 14 September 2011 / Accepted: 21 November 2011 / Published online: 3 December 2011

ABSTRACT

Purpose To study the effectiveness of a peptide targeted nanoglobular Gd-DOTA complexes for MR molecular imaging of prostate cancer in a mouse orthotopic PC-3 prostate cancer model.

Methods A CLT1 (CGLIIQKNEC) peptide-targeted generation 2 nanoglobular Gd-DOTA monoamide conjugate [CLT1-G2-(Gd-DOTA)] was used for imaging fibrin-fibronectin complexes in prostate tumor using a non-specific peptide KAREC modified conjugate, KAREC-G2-(Gd-DOTA) as a control. Cy5 conjugates of CLT1 and KAREC were synthesized for binding studies. Orthotopic PC-3 prostate tumors were established in the prostate of athymic male nude mice. MRI study was performed on a Bruker 7T small animal MRI system.

Results CLT1 peptide showed specific binding in the prostate tumor with no binding in normal tissues. The control peptide had little binding in normal and tumor tissues. CLT1-G2-(Gd-DOTA) resulted in stronger contrast enhancement in tumor tissue than KAREC-G2-(Gd-DOTA). CLT1-G2-(Gd-DOTA) generated ~100% increase in contrast-to-noise ratio (CNR) in the tumor compared to precontrast CNR at 1 min post-injection, while KAREC-G2-(Gd-DOTA) resulted in 8% increase.

Conclusion CLT1-G2-(Gd-DOTA) is a promising molecular MRI contrast agent for fibrin-fibronectin complexes in tumor stroma. It has potential for diagnosis and assessing prognosis of malignant tumors with MRI.

KEY WORDS molecular imaging · MRI · prostate cancer · targeted contrast agent · tumor stroma

INTRODUCTION

Molecular imaging provides a tool to detect and diagnose cancer at the cellular and molecular levels. It not only allows early and accurate tumor localization in diagnostic cancer imaging, but also has a potential to visualize the biological processes of tumor growth, metastasis and response to treatment (1). Magnetic resonance imaging (MRI) is a clinical imaging modality without ionizing radiation. It provides three-dimensional image of the whole body with high resolution. MRI also has a great potential for cancer molecular imaging. In order to achieve effective cancer MR molecular imaging, a sufficient amount of contrast agents should bind to cancer-related biomarkers to generate visible contrast enhancement in MR images. The design and development of novel safe and effective target-specific contrast agents are critical for cancer molecular MRI (2–4). The use of targeted contrast agent can reduce the injected dose, consequently minimize contrast agent related toxic side effect, and improve cancer detection accuracy by ligand-receptor binding.

M. Tan • W. Li • X. Wu • Z.-R. Lu (✉)
Department of Biomedical Engineering, Case Western Reserve University
Wickenden Building, Room 427, 10900 Euclid Avenue
Cleveland, Ohio 44106-7207, USA
e-mail: zxl125@case.edu

M. Tan
Laboratory of Biomedical Material Engineering
Dalian Institute of Chemical Physics, Chinese Academy of Sciences
Dalian 116023, People's Republic of China

S. M. Burden-Gulley • S. M. Brady-Kalnay
Department of Molecular Biology and Microbiology
School of Medicine, Case Western Reserve University
Cleveland, Ohio, USA

D. Lindner
Dept. of Translational Hematology & Oncology Research, Cleveland Clinic
Cleveland, Ohio 44195, USA

V. Gulani • Z.-R. Lu
Department of Radiology, Case Western Reserve University
Cleveland, Ohio 44106, USA

V. Gulani
Department of Urology, Case Western Reserve University
Cleveland, Ohio 44106, USA

Several strategies have been used for the design and development of targeted contrast agents for MR molecular imaging. A commonly used strategy is to target the receptors expressed on the surface of tumor cells using monoclonal antibodies or other targeting ligands (5–8). However, little success has yet been achieved for imaging the biomarkers expressed on the cancer cell surface due to their low concentration in the tumor and low sensitivity of contrast enhanced MRI. The limitations of MRI for molecular imaging may be resolved by proper selection of molecular biomarkers with high local expression in the tissue of interest (9–11). For example, a fibrin-specific contrast agent composed of a small peptide and 4 stable Gd (III) chelates allows high-resolution visualization of acute coronary, cardiac and pulmonary thrombus with MRI (9). The key feature for these agents is that they target the molecular markers abundantly present in the diseased tissue with little presence in normal tissue. A sufficient amount of contrast agent can bind to these targets, resulting in significant contrast enhancement for effective MR molecular imaging.

Tumor stroma comprises of various cancer-related proteins that promote tumor angiogenesis, cancer cell proliferation and metastasis. Some of the proteins have much higher expression in tumor tissue than in normal tissues. These proteins are the promising molecular targets for MR cancer molecular imaging. Fibronectin is abundantly present in the tumor stroma of malignant tumors and forms complexes with other extracellular components, such as fibrin and collagen (12–14). The cancer-related fibrin-fibronectin complexes can be as a potential biomarker in the tumor microenvironment for targeted imaging of prostate cancer. Recently, Ruoslahti and his colleagues reported two cyclic peptides CGLIIQKNEC (CLT1) and CNAGESSKNC (CLT2) specific to fibrin-fibronectin complexes in tumor stroma (15). We have prepared CLT1-(Gd-DTPA) (16) and CLT-1 peptide targeted nanoglobular Gd-DOTA monoamide conjugates (17) as the targeted MRI contrast agents for molecular imaging of the fibrin-fibronectin complexes. Preliminary studies have shown that the peptide targeted contrast agents are effective for cancer MR molecular imaging. Among the tested contrast agents, the generation 2 (G2) targeted nanoglobular Gd-DOTA monoamide conjugate has advantageous features, including relatively high Gd-DOTA content and a size smaller than renal filtration threshold, that warrant further investigation (17). The size of the agent was approximately 5.6 nm, which was small enough to allow effective renal excretion of unbound agent.

In this study, we investigated the effectiveness of the G2 CLT1 targeted nanoglobular Gd-DOTA monoamide conjugate [CLT1-G2-(Gd-DOTA)] for molecular MRI of orthotopic prostate cancer in male mice in comparison with a non-specific peptide modified G2 conjugate KAREC-G2-(Gd-DOTA). The non-specific control agent KAREC-G2-(Gd-DOTA) was prepared by incorporating the non-specific peptide KAREC into the G2 nanoglobular Gd-DOTA monoamide conjugate. The Cy5 conjugates of the peptides were also synthesized for evaluating tumor specific binding. The tumor specific binding of CLT1 peptide was examined in a prostate tumor by fluorescence imaging.

MATERIALS AND METHODS

Synthesis of Peptides and Peptide-Cy5 Conjugates

Peptide CLT1 and non-specific control peptide (KAREC) were synthesized using standard solid phase peptide chemistry from Fmoc-protected amino acids on a 2-chlorotrityl chloride resin. The fluorophore cyanine 5 (Cy5) mono-reactive NHS ester (GE Healthcare Limited, Buckinghamshire, UK) was conjugated to the N-terminus of the peptides with 12-amino-4,7,10-trioxadodecanoic acid as a spacer. The resin was washed three times each with water, N,N-dimethylformamide (DMF), dichloromethane (DCM) and methanol. The CLT1-Cy5 and KAREC-Cy5 conjugates were cleaved from the resin using trifluoroacetic acid (TFA) solution (TFA, 96.5%, triisobutylsilane 1.0% and water 2.5%). The optical probes were dissolved into dimethyl sulfoxide (DMSO) for 2–3 days to allow the formation of disulfide bonds for the cyclic peptide. The final products were purified with high performance liquid chromatography (HPLC) on an Agilent 1100 HPLC system equipped with a ZORBAX 300SB-C18 PrepHT column. The mass (M/z, $M+H^+$) of CLT1-Cy5 was 1960.48 (calculated 1960.86), 1449.30 (calculated 1449.75) for KAREC-Cy5 as determined by MALDI-TOF mass spectrometry.

Peptide-Targeted MRI Contrast Agents

CLT1-G2-(Gd-DOTA) was synthesized by conjugating Gd-DOTA monoamide and CLT1 peptides on the surface of the nanoglobule as described previously (17). A KAREC-G2-(Gd-DOTA), G2 nanoglobular conjugate of KAREC and Gd-DOTA monoamide was similarly prepared. The Gd(III) and sulfur contents were measured by inductively coupled plasma-optical emission spectroscopy (ICP-OES Optima 3100XL, Perkin Elmer, Norwalk, CT). Relaxation rates (R_1 and R_2) of the aqueous solution of the contrast agents at five different concentrations were determined at 1.5T on a Bruker minispec (Bruker Medical GmbH, Ettingen, Germany). Longitudinal and transverse relaxivities (r_1 and r_2) were calculated as the slopes of the linear plots of the relaxation rates *versus* Gd concentration.

Orthotopic Xenograft Prostate Tumor Model

PC-3 human prostate adenocarcinoma cells were purchased from American Type Culture Collection (Manassas, VA) and cultured in RPMI medium supplemented with 5% fetal bovine serum and penicillin/streptomycin/fungizone. The cells were transfected with lentivirus to express green fluorescent protein (GFP) at least 48 h prior to harvesting. NIH athymic male nude mice, age 4–5 weeks, were maintained at the Athymic Animal Core Facility at Case Western Reserve University according to the animal protocols approved by the Institutional Animal Care and Use Committee (IACUC). Mice were anesthetized by intraperitoneal injection of Avertin. A small midline incision was made through the skin and underlying musculature in the abdominal region overlying the bladder. The bladder was reflected through the incision to expose the prostate gland. Approximately 20 μl PC-3-GFP cells (1×10^5 per μl) were injected into the prostate, and the incision was closed with staples.

Fluorescence Imaging of Prostate Tumors

To monitor the growth of the PC-3-GFP prostate tumors, the implanted nude mice were anesthetized by 2% isoflurane and imaged on a Maestro FLEX *In Vivo* Imaging System (Cambridge Research & Instrumentation, Inc. Woburn, MA, USA) after cell injection. Spectral fluorescence images were obtained using the appropriate filters for GFP (excitation: 444–490 nm; emission: 515 nm long-pass filter; acquisition settings: 500–720 in 10 nm steps) and Cy5 (excitation: 576–621 nm; emission: 635 nm long-pass filter; acquisition settings: 630–800 in 10 nm steps). Acquisition setting was 15 ms for GFP and 100 ms for either CLT1-Cy5 or KAREC-Cy5 (exposure times were automatically calculated). GFP fluorescent images were acquired at different time points after cancer inoculation.

To assess binding, background images were acquired before injection of the peptide probes. The mice bearing orthotopic PC-3 prostate xenograft tumors were intravenously injected with CLT1-Cy5 or KAREC-Cy5 via a tail vein at a dose of 333 nmol/kg. After 2 h, allowing for clearance of unbound peptides, the mice were sacrificed and the tumors and various organs were imaged on the Maestro FLEX *In Vivo* Imaging System. The Cy5 signal was spectrally extracted from the multispectral fluorescence images with Maestro software (Cambridge Research & Instrumentation, Inc, Woburn, MA) after subtracting the background auto-fluorescence. Regions of interest (ROIs) were selected over the tumors and organs. Average signal values in tumor ROIs were normalized to the non-tumor ROI. Statistical analysis was performed using Origin 8 software (Origin Lab Corp.).

In Vivo MR Imaging

The MRI study was performed on a Bruker Biospec 7T MRI scanner (Bruker Corp., Billerica, MA, USA) with a volume radio frequency (RF) coil. The mice were randomly divided into groups (4 for each agent) 3 weeks after tumor cell inoculation for the MR molecular imaging study. The tumor size is about 3–5 mm in diameter. Animals were anesthetized with 2% isoflurane supplemented with O_2 during the imaging experiment *via* a nose cone. Electrodes were attached to front paws and right leg for electrocardiography (ECG) monitoring through an MR-compatible small animal gating and monitoring system (SA Instruments, Stony Brook, NY). The anesthetized animals' body temperature was maintained at 35 ± 1°C by blowing hot air into the magnet through a feedback control system. The heat flow and the anesthesia level were manually adjusted to maintain the heart rate close to that under conscious conditions. A 30-gauge needle was inserted into the tail vein and connected to a syringe through flexible plastic tubing (Tygon®, Saint-Gobain PPL Corp. Akron, OH) for injecting contrast agents. MRI contrast agents were administered in the tail vein at a dose of 0.03 mmol-Gd/kg. The mice were scanned before injection and at 1, 6, 12, 18, 24, 30, 36, 42, and 50 min post-injection using *multi-slice multi-echo* (MSME) T_1-weighted MRI sequence. The acquisition parameters were 500/14 ms TR/TE, 90° flip angle, 2 averages, 4 min 16 s acquisition time, 2.0 mm slice thickness, 9.06 cm field of view, 256×256 matrix size, 15 slices. Image analysis was performed by using Bruker ParaVision 4.0 imaging software. ROI was drawn over the whole tumor in the two-dimensional imaging plane and average signal intensity was measured. The contrast to noise ratio (CNR) was calculated using the following equation: $\mathrm{CNR} = (S_t - S_m)/\sigma_n$; where S_t (tumor) and S_m (muscle) denote the signal within ROIs and σ_n is the standard deviation of noise measured from the background noise in the same slice. Statistical analysis was performed using a two-way ANOVA with Bonferroni's test, assuming statistical significance at $p<0.05$.

Histochemical Analyses

Mice bearing PC-3 GFP-expressing prostate tumor tissues were injected with CLT1-Cy5 or KAREC-Cy5 via a tail vein at a dose of 10 nmol/mouse. The mice were sacrificed 2 h later and tumor tissues were collected and cryosectioned into 5-μm slices. The slices were rinsed with PBS, coverslipped with UltraCruz™ mounting medium (sc-24941, Santa Cruz Biotechnology, Inc. Santa Cruz, CA, USA) containing 4′,6-diamidino-2-phenylindole (DAPI) and imaged immediately at 20X on an Olympus FV1000 confocal laser scanning microscope. The scanning resolution was 512×512 pixels with a scan rate of 2.7 s/frame, while the laser excitation

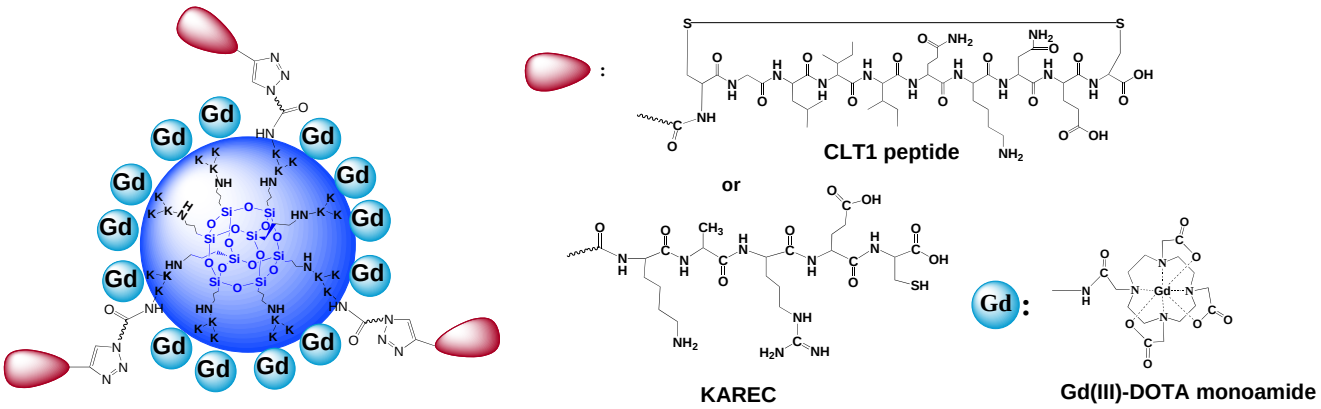

Fig. 1 Chemical structures of CLT1-G2-(Gd-DOTA) and KAREC-G2-(Gd-DOTA). K represents lysine.

wavelength and optical light path and filters were set for the designated fluorescent label (DAPI was excited using the 405-nm laser; GFP was excited using the 488-nm laser; Cy5 was excited with the 635-nm laser). The images were processed with the Olympus FV software.

RESULTS

Contrast Agents

The structures of CLT1 and KAREC modified generation 2 nanoglobule (poly-*L*-lysine dendrimer with a silsesquioxane cubic core) Gd-DOTA monoamide conjugates, CLT1-G2-(Gd-DOTA) and KAREC-G2-(Gd-DOTA), are shown in Fig. 1. KAREC-G2-(Gd-DOTA) was prepared as the non-targeted control agent (18). The sulfur and Gd(III) content in the conjugates were determined by ICP-OES to calculate the peptide and Gd-DOTA content in the conjugates. On average, 3 CLT1 peptides and 4 control peptides were conjugated to the G2 nanoglobular contrast agents, respectively. Approximately 20 Gd-DOTA chelates were conjugated to the nanoglobular agents. The physicochemical parameters of the contrast agents are listed in Table I. The r_1 and r_2 relaxivities of the targeted agent were 11.6 and 15.7 mM^{-1} s^{-1} per Gd(III) chelate at 1.5T, and 11.4 and 15.4 mM^{-1} s^{-1} per Gd(III) chelate for the control agent. Both peptide modified nanoglobular contrast agents have similar physicochemical properties. Therefore, KAREC-G2-(Gd-DOTA) is an appropriate control for CLT1-G2-(Gd-DOTA) for molecular MRI. CLT1-Cy5 and KAREC-Cy5 were synthesized by solid phase chemistry to study their specific binding to prostate tumor. The structure of the Cy5 labeled peptides was characterized by MALDI-TOF mass spectrometry.

Fluorescent Imaging of Prostate Tumors

Figure 2 shows the GFP fluorescence images of a live mouse and the prostate tumor after the mouse was sacrificed 3 weeks after PC3 cancer cell inoculation. The GFP expressing tumor was visible in the fluorescence image of the live mouse and located close to the bladder. The presence of tumor in the prostate was further confirmed by GFP fluorescence imaging after dissection, which indicated the tumor location below the bladder and in front of the rectum in this mouse. The binding specificity of CLT1 peptide to the PC3 tumor was investigated by fluorescence imaging using CLT1-Cy5 with KAREC-Cy5 as a non-targeted control. Figure 3 shows the bright-field and fluorescent images of the major organs and tissues from the mice injected with the probes 2 h after the injection. The GFP-expressing tumor tissues exhibited intense green fluorescence. Strong red fluorescence was shown in the prostate tumor from the mouse injected with CLT1-Cy5, whereas little fluorescence was detected in the tumor with KAREC-Cy5. No Cy5 fluorescence was observed in healthy organs

Table I Physicochemical Properties of the Nanoglobular MRI Contrast Agents

Contrast agents	Gd content mmol-Gd/g dendrimer	No. of Gd-DOTA-monoamide chelates	No. of surface peptide	Molecular weight	r_1 /r_2 [mM^{-1}(Gd)s^{-1}] at 1.5T
Targeted	1.18	20/32	~3	27,000	11.6/15.7
Control	1.16	20/32	~4	26,700	11.4/15.4

Targeted: CLT1-G2-(Gd-DOTA); Control: KAREC-G2-(Gd-DOTA)

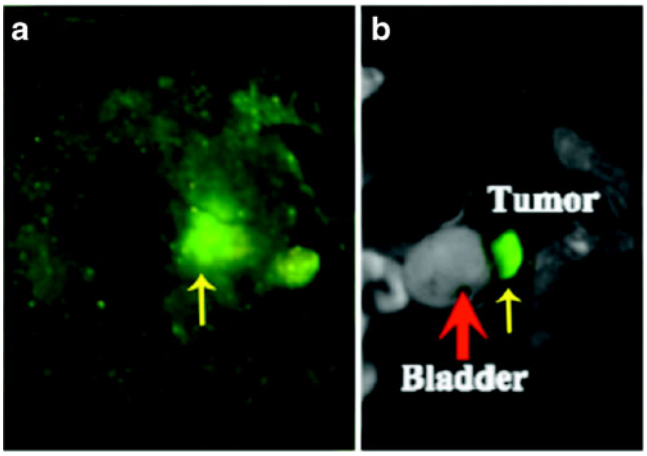

Fig. 2 Fluorescent images showing the presence of GFP-expressing PC-3 prostate tumor in a live mouse (**a**) and after sacrificing the mouse (**b**). The images were acquired 3 weeks after PC3 cancer cell inoculation. *Red thick arrow* points to the bladder and *yellow thin arrow* points to the tumor.

and tissues except the kidneys with either the targeted or control probe. Significant red fluorescence was shown in the kidneys because kidneys are the main organs for excretion and it might take a relatively long time for complete clearance from the kidneys. CLT1-Cy5 specifically bound to the prostate tumor tissue with little non-specific binding in normal tissues. Figure 4 shows the side-by-side comparison of the tumors injected with CLT1-Cy5 and KAREC-Cy5. Fluorescence intensity in orthotopic tumors of the mice injected with CLT1-Cy5 was 7.7 times greater than in the mice injected with KAREC-Cy5.

In Vivo MR Imaging

T_1-weighted 2D MR images of the tumor bearing mice contrast enhanced with CLT1-G2-(Gd-DOTA) and KAREC-G2-(Gd-DOTA) are shown in Fig. 5. Substantial enhancement of the fluid in the urinary bladder was observed starting at 6 min after the administration of the contrast agents, and continued accumulation of strongly enhancing fluid in the bladder enhancement was observed to the end of the experiment. CLT1-G2-(Gd-DOTA) resulted in strong enhancement in the tumor tissue, particularly in the tumor periphery, at 1 min post-injection. The enhancement gradually decreased over time after injection, but substantial enhancement was still visible at 50 min post-injection. Much less enhancement was observed in the tumor with KAREC-G2-(Gd-DOTA) at 1 min post-injection. The tumor size was in the range of 3–5 mm in diameter as estimated from the MR images with Bruker ParaVision 4.0 imaging software. The tumor location was in accordance with that observed by fluorescence imaging.

Quantitative analysis of MR signal in the tumor revealed that CLT1-G2-(Gd-DOTA) resulted in approximately 100% increase in contrast-to-noise ratio (CNR) in the tumor as compared to precontrast CNR at 1 min post-injection, while KAREC-G2-(Gd-DOTA) only result in 8% CNR increase (Fig. 6). CLT1-G2-(Gd-DOTA) exhibited significantly higher tumor CNR than the control agent in the first 25 min ($p < 0.05$). The tumor CNR gradually decreased over time possibly due to the dissociation of the agent from the target. CLT1-G2-(Gd-DOTA) still resulted in 30% CNR

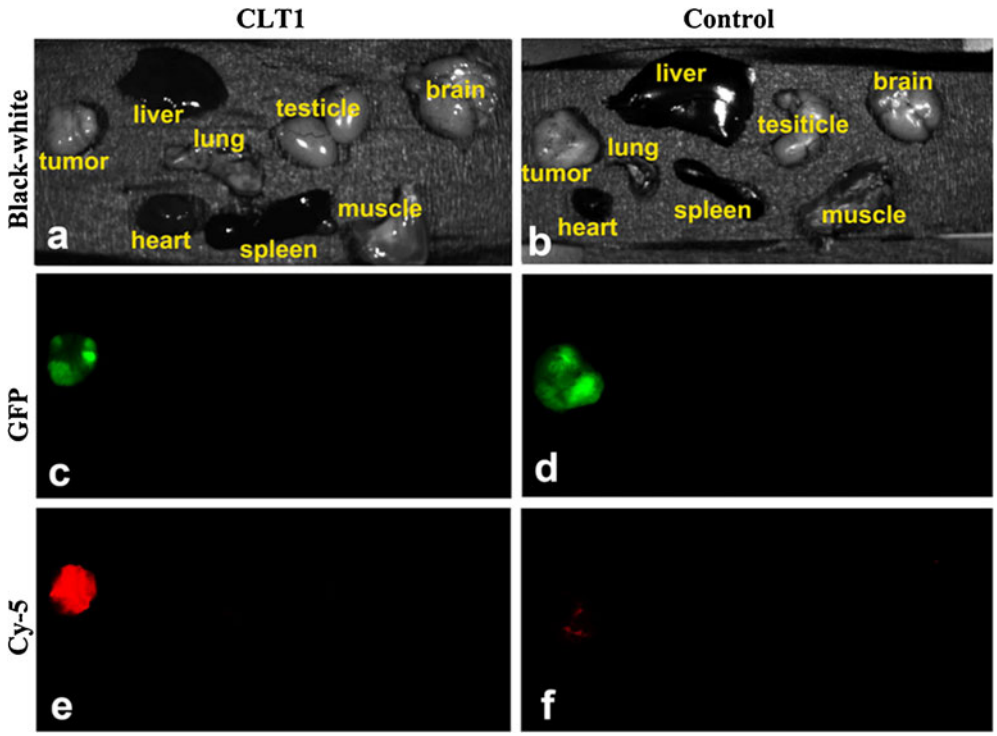

Fig. 3 Mice bearing orthotopic PC-3-GFP prostate cancer xenografts were intravenously injected with CLT1-Cy5 or KAREC-Cy5. After 2 h for the clearance of unbound peptide, the mice were sacrificed and the tumors and various organs were imaged with the Maestro FLEX *In Vivo* Imaging System. Brightfield images of tumors and various organs of the mouse injected with CLT1-Cy5 (**a**) or KAREC-Cy5 (**b**) are shown. GFP fluorescence was observed in tumors but not other organs and tissues from these mice (**c**, **d**). Cy5 fluorescence was much greater in the tumor from the mouse injected with CLT1-Cy5 (**e**) than from the mouse injected with KAREC-Cy5 (**f**).

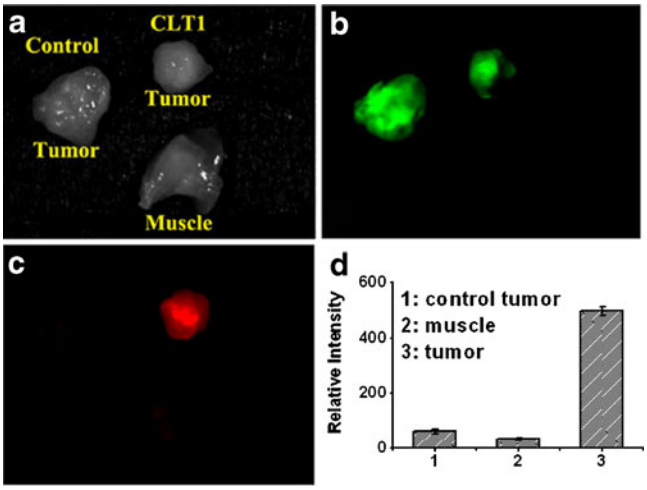

Fig. 4 Tumors of mice injected with CLT1-Cy5 or KAREC-Cy5 and normal tissue muscle were imaged side by side with the Maestro FLEX *In Vivo* Fluorescence Imaging System. Exposure time was 11 ms for GFP and 96 ms for the optical probes. Brightfield image of tumors from mice injected with CLT1-Cy5, KAREC-Cy5 and normal muscle is shown (**a**). Fluorescence images of the tissues indicate that GFP expression is limited to tumor tissues (**b**) and Cy5 fluorescence is much greater in tumor from the mouse injected with CLT1-Cy5 than KAREC-Cy5 (**c**). CLT1-Cy5 showed much higher specific binding in the tumor tissue than the control (**d**).

increase at 50 min after injection as compared to the pre-contrast CNR. The CNR with KAREC-G2-(Gd-DOTA) did not change significantly during the period of the experiment. Since the r_1 relaxivity of both agents was very similar, the specific binding of CLT1-G2-(Gd-DOTA) resulted in strong enhancement in tumor as compared to KAREC-G2-(Gd-DOTA) or to normal tissue.

Histological Analysis

Figure 7 shows the fluorescent images of tumor sections from mice injected with CLT1-Cy5 and KAREC-Cy5. The DAPI bound to the DNA in cell nuclei showed blue fluorescence. The GFP labeled tumor tissues showed strong green fluorescence. Strong red fluorescence of Cy5 was observed in the tumor sections from the mice injected with CLT1-Cy5, while little Cy5 fluorescence was shown in the tissue section from the mice injected with KAREC-Cy5. The merged fluorescent images exhibited good correlation of green fluorescence from the tumor cells and red fluorescence from CLT1-Cy5. The result indicates specific binding of CLT1-Cy5 in the tumor tissue after intravenous administration of the agent.

DISCUSSION

Prostate cancer is common among men over 50 years old. If untreated, prostate cancer can metastasize and become untreatable (18). Early and accurate detection and diagnosis of prostate cancer are critical for the treatment and management of prostate cancer. Molecular imaging of the biomarkers in prostate cancer will be a valuable tool for the diagnosis and prognosis of prostate cancer (19,20). It is well documented that the cancer related fibronectin is highly expressed in malignant tumors and rarely present in normal adult tissues, including prostate cancer (13,21). Fibronectin forms complexes with fibrin and collagen in the extracellular matrix. CLT1 peptide was developed for targeting the fibrin-fibronectin complexes in tumor stroma (18). *In vivo* fluorescence imaging verified the specific binding of CLT1 peptide to the orthotopic prostate tumor tissue. The high tumor specificity of CLT1 peptide is ideal for the design of targeted contrast agents for MR cancer molecular imaging. As compared to monoclonal antibodies and their fragments, the peptide has a small size and can readily diffuse into tumor tissues for effective target binding and molecular imaging. The small size also allows unbound contrast agents to be eliminated from the body via renal filtration to reduce background signal and to minimize the accumulation of Gd (III) chelates in normal tissues. Complete elimination of the Gd(III) based MRI contrast agents from the body is critical for minimizing the possibility of potential toxic side effects related to their slow excretion, including nephrogenic systemic fibrosis observed in a small number of patients with severely impaired renal function.

The size of the peptide-targeted nanoglobular MRI contrast agent (5.6 nm) was smaller than the renal filtration threshold (ca. 8.0 nm). The unbound peptide was readily

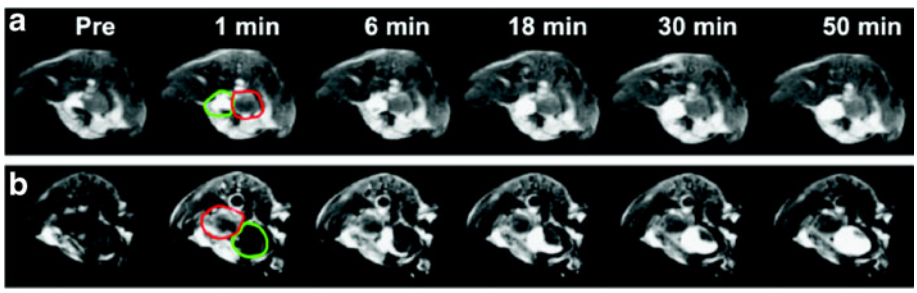

Fig. 5 Representative 2D axial T_1-weighted MR images of a prostate tumor bearing mouse before (pre) and at 1, 6, 18, 30, 50 minutes after the injection of the KAREC-G2-(Gd-DOTA) (**a**) and CLT1-G2-(Gd-DOTA) (**b**) at 0.033 mmol-Gd/kg. The tumor is *circled* with *red color* and the bladder with *green*.

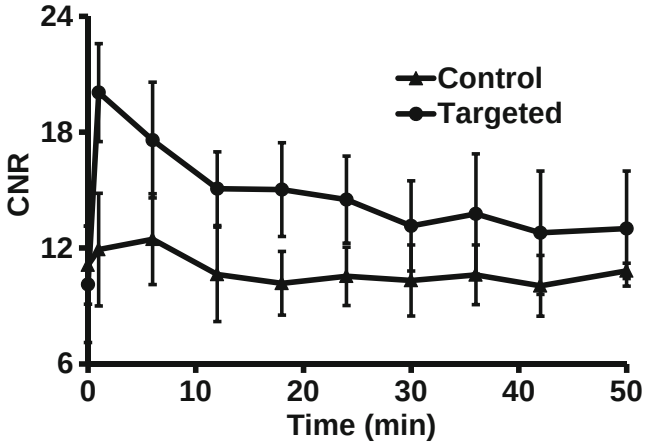

Fig. 6 Contrast-to-noise ratio (CNR) in the tumor with CLT1-G2-(Gd-DOTA) and KAREC-G2-(Gd-DOTA) administered at 0.033 mmol-Gd/kg in the orthotopic prostate tumor bearing mice ($N=4$). * $p < 0.05$.

excreted via renal filtration and accumulated in the urinary bladder as shown in Fig. 5. Rapid elimination of the unbound contrast agent from the body is critical to minimize the potential toxic side effects associated with Gd-based contrast agents. No sign of toxicity was observed in the mice after the injection of the contrast agents and a few days after the study. Nevertheless, comprehensive toxicological studies are needed before clinical development of the targeted contrast agent.

The targeted contrast agent CLT1-G2-(Gd-DOTA) resulted in strong tumor enhancement in the periphery of orthotopic prostate cancer as early as 1 min post-injection. The enhancement in the tumor was heterogeneous, with stronger enhancement in the tumor periphery than in tumor core. However, the fluorescence image in Fig. 4 showed relatively uniform distribution of CLT1-Cy5 in the tumor, because the fluorescence image was the image of tumor surface, while the MR image was the cross-section image. The MRI enhancement pattern was also different from what was previously observed in the mouse flank breast tumor. Relatively uniform enhancement was observed across tumor tissue of the flank model with CLT1-G2-(Gd-DOTA) (17). This disparity in enhancement pattern is possibly attributed to the difference between flank tumor model and orthotopic tumor model. Flank tumor xenografts are more angiogenic and more aggressive tumor models than orthotopic tumors. Orthotopic tumor models are closer to the naturally developed tumors.

Molecular imaging has been proven successful in detection and diagnosis of prostate cancer in clinical practice with imaging modalities of high sensitivity, including PET and SPECT (22–25). Unfortunately, these imaging modalities cannot effectively visualize anatomic structures. They are often combined with other structural imaging modalities, *e.g.* CT and MRI, to correlate molecular imaging with structural imaging to improve diagnostic accuracy (22–25). Although dual imaging modalities, including PET/CT and SPECT/CT, have enjoyed great success in combining molecular imaging with anatomic imaging in clinical practice, it would be ideal to use a single imaging modality for both effective molecular imaging and anatomic imaging of cancer and to reduce both unnecessary exposure to ionizing radiation and the cost. We have shown in this study that it is possible to achieve both molecular imaging and anatomic imaging in one imaging modality with contrast enhanced MRI. Although MRI has lower sensitivity than nuclear medicine for molecular imaging, effective MR molecular imaging can be achieved with proper selection of molecular targets and targeted MRI contrast agents. Fibrin-fibronectin complexes are abundantly present in the extracellular matrix of the orthotopic prostate tumor. A sufficient amount of CLT1 targeted contrast agent binds to the molecular target to generate MR signal enhancement detectable by MRI.

In conclusion, this study has demonstrated that CLT1-G2-(Gd-DOTA) is effective for MR molecular imaging of prostate cancer in a mouse orthotopic prostate cancer model. Contrast enhanced MRI with CLT1-G2-(Gd-DOTA) is promising for molecular imaging of cancer related fibrin-

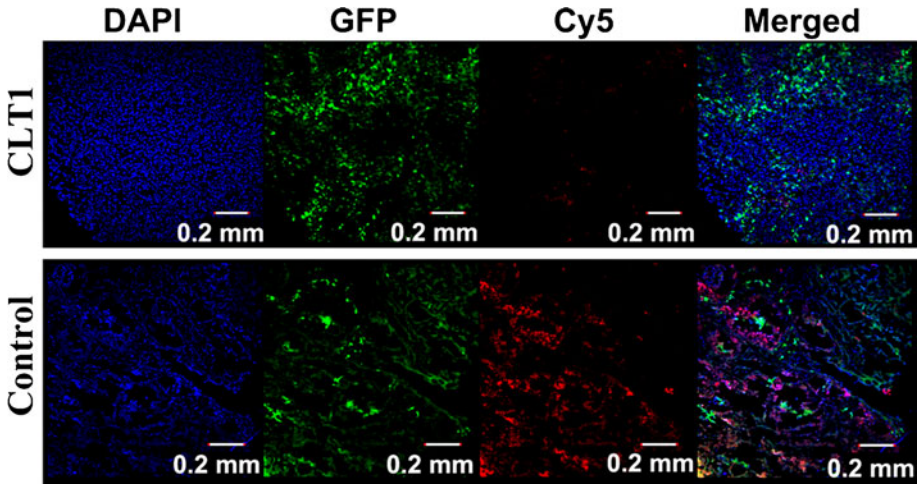

Fig. 7 Histological analysis of tumor tissue injected with 10 nmol of CLT1-Cy5 or KAREC-Cy5.

fibronectin complexes in the tumor stroma of the orthotopic prostate tumor model with high anatomic resolution. It has a potential for accurate diagnosis of malignant tumors. Further preclinical studies are needed to demonstrate the safety of the targeted contrast agent to warrant further clinical development of the agent.

ACKNOWLEDGMENTS & DISCLOSURES

This work is supported in part by the NIH R01 CA097465 and a J&J-CWRU Innovation Challenge grant. We greatly appreciate Drs. Xin Yu, Ya Chen and Yong Chen for their technical assistance in MRI data acquisition. In addition, Mrs. Yvonne Parker provided expert technical assistance in the production of orthotopic tumor xenografts. We thank James P. Basilion for use of the Maestro Imaging System.

REFERENCES

1. Weissleder R. Molecular imaging in cancer. Science. 2006;312:1168–71.
2. Yallapu MM, Foy SP, Jain TK, Labhasetwar V. PEG-functionalized magnetic nanoparticles for drug delivery and magnetic resonance imaging applications. Pharm Res. 2010;27:2283–95.
3. Cheng Z, Thorek DL, Tsourkas A. Gadolinium-conjugated dendrimer nanoclusters as a tumor-targeted T1 magnetic resonance imaging contrast agent. Angew Chem Int Ed Engl. 2010;49:346–50.
4. Pan D, Caruthers SD, Chen J, Winter PM, Senpan A, Schmieder AH, Wickline SA, Lanza GM. Nanomedicine strategies for molecular targets with MRI and optical imaging. Future Med Chem. 2010;2:471–90.
5. Sipkins DA, Cheresh DA, Kazemi MR, Nevin LM, Bednarski MD, Li KC. Detection of tumor angiogenesis *in vivo* by $\alpha_v\beta_3$-targeted magnetic resonance imaging. Nat Med. 1998;4:623–6.
6. Curtet C, Maton F, Havet T, Slinkin M, Mishra A, Chatal JF, Muller RN. Polylysine-Gd-DTPAn and polylysine-Gd-DOTAn coupled to anti-CEA $F(ab')_2$ fragments as potential immunocontrast agents. Relaxometry, biodistribution, and magnetic resonance imaging in nude mice grafted with human colorectal carcinoma. Invest Radiol. 1998;33:752–61.
7. Ke T, Jeong E, Wang X, Feng Y, Parker D, Lu Z. RGD targeted poly(L-glutamic acid)-cystamine-(Gd-DO3A) conjugate for detecting angiogenesis biomarker alpha(v)beta(3) integrin with MRT1 mapping. Int J Nanomed. 2007;2:191–9.
8. Artemov D, Mori N, Ravi R, Bhujwalla Z. Magnetic resonance molecular imaging of the HER-2/neu receptor. Cancer Res. 2003;63:2723–7.
9. Caravan P, Das B, Dumas S, Epstein FH, Helm PA, Jacques V, Koerner S, Kolodziej A, Shen L, Sun WC, Zhang Z. Collagen-targeted MRI contrast agent for molecular imaging of fibrosis. Angew Chem Int Ed Engl. 2007;46:8171–3.
10. Boutry S, Burtea C, Laurent S, Toubeau G, Vander Elst L, Muller RN. Magnetic resonance imaging of inflammation with a specific selectin-targeted contrast agent. Magn Reson Med. 2005;53:800–7.
11. Sirol M, Fuster V, Badimon JJ, Fallon JT, Moreno PR, Toussaint JF, Fayad ZA. Chronic thrombus detection with *in vivo* magnetic resonance imaging and a fibrin-targeted contrast agent. Circulation. 2005;112:1594–600.
12. Santimaria M, Moscatelli G, Viale GL, Giovannoni L, Neri G, Viti F, Leprini A, Borsi L, Castellani P, Zardi L, Neri D, Riva P. Immunoscintigraphic detection of the ED-B domain of fibronectin, a marker of angiogenesis, in patients with cancer. Clin Cancer Res. 2003;9:571–9.
13. Sönmez H, Süer S, Karaarslan I, Baloğlu H, Kökoğlu E. Tissue fibronectin levels of human prostatic cancer, as a tumor marker. Canc Biochem Biophys. 1995;15:107–10.
14. Kaspar M, Zardi L, Neri D. Fibronectin as target for tumor therapy. Int J Cancer. 2006;118:1331–9.
15. Pilch J, Brown D, Komatsu M, Järvinen TA, Yang M, Peters D, Hoffman RM, Ruoslahti E. Peptides selected for binding to clotted plasma accumulate in tumor stroma and wounds. Proc Natl Acad Sci U S A. 2006;103:2800–4.
16. Ye F, Jeong E, Jia Z, Yang T, Parker D, Lu Z. A peptide targeted contrast agent specific to fibrin-fibronectin complexes for cancer molecular imaging with MRI. Bioconjugate Chem. 2008;19:2300–3.
17. Tan M, Wu X, Jeong E, Chen Q, Lu Z. Peptide-targeted nanoglobular Gd-DOTA monoamide conjugates for magnetic resonance cancer molecular imaging. Biomacromolecules. 2010;11:754–61.
18. Mahato R, Qin B, Cheng K. Blocking IKKα expression inhibits prostate cancer invasiveness. Pharm Res. 2011;28:1357–69.
19. Lee CM, Jeong HJ, Cheong SJ, Kim EM, Kim DW, Lim ST, Sohn MH. Prostate cancer-targeted imaging using magnetofluorescent polymeric nanoparticles functionalized with bombesin. Pharm Res. 2010;27:712–21.
20. Wu X, Feng Y, Jeong EK, Emerson L, Lu ZR. Tumor characterization with dynamic contrast enhanced magnetic resonance imaging and biodegradable macromolecular contrast agents in mice. Pharm Res. 2009;26:2202–8.
21. Işisağ A, Neşe N, Ermete M, Lekili M, Ayhan S, Kandiloğlu AR. Col IV and Fn distribution in prostatic adenocarcinoma and correlation of 67LR, MMP-9 and TIMP-1 expression with Gleason score. Anal Quant Cytol Histol. 2003;25:263–72.
22. Desai B, Elatre W, Quinn DI, Jadvar H. FDG PET/CT demonstration of pancreatic metastasis from prostate cancer. Clin Nucl Med. 2011;36:961–2.
23. Pinkawa M, Eble MJ, Mottaghy FM. PET and PET/CT in radiation treatment planning for prostate cancer. Expert Rev Anticancer Ther. 2011;11:1035–41.
24. Rieter WJ, Keane TE, Ahlman MA, Ellis CT, Spicer KM, Gordon LL. Diagnostic performance of In-111 capromab pendetide SPECT/CT in localized and metastatic prostate cancer. Clin Nucl Med. 2011;36:872–8.
25. Schuster DM, Savir-Baruch B, Nieh PT, Master VA, Halkar RK, Rossi PJ, Lewis MM, Nye JA, Yu W, Bowman FD, Goodman MM. Detection of recurrent prostate carcinoma with anti-1-amino-3-18F-fluorocyclobutane-1-carboxylic acid PET/CT and 111In-capromab pendetide SPECT/CT. Radiology. 2011;259:852–61.